Retrieval of Snow Properties from AVIRIS Data

Anne W. Nolin and Jeff Dozier

Center for Remote Sensing and Environmental Optics
The University of California
Santa Barbara, California

Abstract. A map of snow surface-layer grain size was produced and determination of thin snow areas was made using image data collected over the Sierra Nevada, California by the Airborne Visible/Infrared Imaging Spectrometer (AVIRIS). Quantitative estimates of snow grain size were formulated based on 1990 data collected over Mammoth Mountain. Because reflectance is sensitive to ice grain size in the near-infrared wavelengths, a single AVIRIS band, centered at 1.05 μm, was used. The AVIRIS data were atmospherically corrected to surface reflectance. A two-stream radiative transfer model was then used to formulate the relationship between grain size and snowpack reflectance for a wide range of ice sphere radii. A piecewise linear mapping provided a means for inverting the image data from reflectance to optically equivalent grain size. The color-coded grain size map illustrates the distribution of grain sizes over the Mammoth Mountain area. There is some correspondence between solar illumination angle and estimated grain size. Applying a spectral mixture model to a multi-band image of the area generated a "shade" component image which may aid in providing a correction factor for those snow-covered pixels which were not fully illuminated. Spectral mixture analysis was also used to map regions of thin snow using a 1989 Tioga Pass AVIRIS image. Using five spectral endmembers derived from the image, we were able to map thin snow, thick snow, water, rock/soil and vegetation.

I. Introduction

Recent research in the area of snow science has examined the hydrologic, climatologic and hydrochemical significance of seasonal snowpacks. While snow hydrologists have long been involved in determining the quantity of water held by the snowpack and the timing of melt, of newly found importance is the hydrochemical process of chemical elution from the snowpack and its effects on the aquatic ecology of alpine watersheds. Accurate assessment of the metamorphic state of the pack, as determined by changes in snow grain size, and of the timing and spatial distribution of snowmelt will help us understand the important hydrochemical processes in seasonal snowmelt.

Because snow is one of the brightest natural substances of great extent on this planet, it also plays a significant role in the global energy balance. Accurate parameterization of the temporal and spatial changes in surface albedo of seasonally snow-covered areas is essential for accuracy in climate models since these models require snow albedo values as as a lower boundary condition.

In this paper, we examine a technique for identifying areas of thin snow in an AVIRIS scene and we discuss the basis for, and show the preliminary results of, an inversion technique for mapping snow grain size using AVIRIS imagery.

II. Mapping Thin Snow Areas

One of the main problems in the remote sensing of snowpack properties has been the inability to distinguish between thin snow case and "dirty" snow since both have decreased albedo when compared to pure, thick snow. While the case of snow containing appreciable amounts of absorbing impurities (such as dust and soot) is an important area of investigation, in this paper we will will only be examining a technique for mapping of optically thin snow.

An optically thin snow is one whose reflectance is reduced by the effects of the underlying substrate such as rock or soil by at least 1% when compared to a very deep (optically semi-infinite) snowpack. Because the optical thickness of a snowpack varies with wavelength and with snow grain size, density, and physical depth, it is helpful to to express the minimum thickness of an optically semi-infinite snowpack in terms of snow water equivalence. For a solar zenith angle of 60°, Table 1 (from Dozier et al., 1989) shows the minimum values in millimeters of water equivalence.

TABLE 1. Snow-Water Equivalence (mm) of Semi-Infinite Snow Pack

λ	grain radius (μm)		
(μm)	50	300	1000
0.45	17	63	145
0.7	10	37	80
0.9	5	15	30
1.6	< 1	< 1	1

This table shows two things: first, that shorter wavelengths are transmitted farther and therefore more snow is needed for a snowpack to be semi-infinite, and, second, that when a snowpack comprises smaller ice grains, there are more scattering events so less snow is needed in order for it to behave as though it were semi-infinite. Therefore, estimates of grain size and snow water equivalence are needed to assess the effects of optically thin snow on albedo.

A 1989 AVIRIS image of the Tioga Pass region of the Sierra Nevada, California was used for this part of the work because it contained a fairly large 3 km by 3 km flat area with patchy thin snow adjacent to Tioga Lake. Concurrent ground truth measurements and snow stereologic measurements provided values for snow depth, grain size and density. Spectral mixture analysis was used to discriminate between areas of deep snow, thin snow, and bare ground in the image. This linear-mixing approach (Adams et al., 1989; Smith et al., 1990) can be used to generate fraction images and show relative abundances of spectral endmembers.

$$DN_c = \sum_{i=1}^{N} F_i \, DN_{i,c} + E_c \qquad (1)$$

where, DN_c is the radiometrically calibrated radiance in AVIRIS channel c.

F_i is the fraction of endmember i.

$DN_{i,c}$ is the radiance of endmember i in channel c.

N is the number of spectral endmembers.

E_c is the error for channel c of the fit of N spectral endmembers.

First, endmembers were selected using a 3-band color-composite AVIRIS image; these endmembers were water, thin snow, thick snow, rock/soil, and vegetation. The mixing algorithm was then applied to the AVIRIS data and endmember fractions were displayed. Slide 26 shows thick snow (dark blue), thin snow (light blue) and vegetation (green) and water (black) . Ground measurements indicate that thin snow depths ranged from .25 m to 1.25 m and thicker snowpack depths were as great as 2.5 m. Concurrent PIDAS (Portable Instantaneous and Display and Analysis Spectrometer) reflectance measurements showed that for the thinnest snowpack (SWE = .11 m) the soil substrate influenced the magnitude and shape of the snow spectral reflectance curve (Nolin et al., 1990). To provide a measure of the "fit" of the endmembers to the AVIRIS data, the root-mean-square (RMS) of the error for each channel was calculated. RMS values were displayed as DNs with higher DN corresponding to a greater RMS error. Although RMS DNs were as high as 12 in parts of the image, this was probably due to the fact that no shade endmember was used to in the spectral mixture analysis. There were no well-shaded pixels in the image and although water could have been used as a spectral proxy for shade, water was a separate endmember and so was not used to simulate shade. Also, non-linearities introduced from several sources reduced the accuracy of the outcome. These non-linearities are due to adjacency effects of bright pixels next to dark pixels adding some unaccounted-for path radiance, to the bidirectional reflectance effects of snow which are not considered here, and to the fact that snow in this region is also an intimate mixture of ice and absorbing impurities which cannot be modeled as a linear mixture. However, the fact remains that thin snow areas are easily discriminated from optically thick snowpacks in this AVIRIS image.

III. Grain size inversion model

The basis of the inversion approach used to obtain estimates of snow grain radii is fact that through the near-infrared portion of the spectrum, ice becomes is moderately absorbing. Figure 1 (from Dozier, 1989) shows that in the 0.9 μm to 1.3 μm region, snowpack reflectance is very sensitive to ice grain size. In contrast to the relatively deep transmission of visible wavelengths into the snowpack, this near-infrared absorption occurs over a vertical range in the snowpack on the order of millimeters. Warren and Wiscombe (1980) noted that increased grain size was primarily responsible for lower values of shortwave, spectrally integrated albedo.

To relate the optical properties of snowpacks to physical properties such as grain size, we rely on radiative transfer models. By making the assumption of spherically shaped ice crystals, the problem becomes far easier to calculate. The equivalent sphere is the one which has the same volume-to-surface ratio as the ice grain. For randomly oriented moderately non-spherical scatterers this is valid (Mugnai and Wiscombe, 1980) but this assumption may not hold for very new snow and oriented snow microstructure. The scattering properties for an ice sphere of appropriate radius r can be calculated by the Mie equations, the complex angular momentum approximation or, for larger grains, by geometric optics. Then the radiative transfer equation can be used to calculate the multiple scattering and absorption of the incident radiation. This is represented by:

$$\mu \frac{dL(\tau, \mu, \phi)}{d\tau} = -L(\tau, \mu, \phi) + J(\tau, \mu, \phi) \quad (2)$$

where, L is radiance at optical depth τ in direction θ, ϕ; ϕ is the azimuth; θ is the angle from zenith; and $\mu = \cos\theta$. J is the source function; it results from scattering of both direct and diffuse radiation or, at thermal wavelengths, emission. The spectral reflectance for direct and diffuse irradiance can thus be modeled from a knowledge of the snow's physical properties.

Given the Mie scattering parameters for spherical ice grains ranging in size from 40 μm to 2500 μm as input, a two-stream radiative transfer model calculated reflectances for each grain size at a wavelength of 1.05 μm. Figure 2 shows the relationship between grain size and reflectance as determined by the model. The wavelength, 1.05 μm, was chosen because it is in a spectral region where reflectance is particularly sensitive to grain radius size. There is also little atmospheric absorption in that region so that atmospheric correction of AVIRIS data is relatively low-error. A piecewise linear mapping was implemented to transform the modeled data to functions which could relate a reflectance value from the AVIRIS image to an optically equivalent grain radius.

Conversion of AVIRIS spectral radiance to surface reflectance was performed using LOWTRAN7 and a two-stream model. Running LOWTRAN7 with the parameters for a midlatitude winter atmosphere and with a visibility of 150 km, values of transmittance (T), single-scattering albedo ($\tilde{\omega}$), and asymmetry parameter (g) were generated. Atmospheric spectral transmittance was converted to optical thickness (τ = -log(T)), and these parameters, τ, ω, and g, were used to drive a radiative transfer model to obtain direct and diffuse irradiance at the surface and upwelling irradiance (Dubayah, 1990).

Next, application of a table look-up procedure using the reflectance-to-grain size relationships provided the conversion from a reflectance image to one which was a map of optically equivalent ice grain radii. Pixels whose values fell outside of the range of reflectances which could be mapped as ice grains were masked from the image (values set to zero). Note that these are optically equivalent (same volume-to-surface ratio) grain radii for ice grains comprising the surface layer of the snowpack and do not represent a depth-averaged grain size for the snowpack.

Slide 27 shows a single-band image of grain size which has been colored to show three distinct size categories of ice grains. North is to the lower left of the image, illumination by the sun is from the upper right of the image; the solar zenith angle for that date and time was 31°. Mammoth Mountain occupies the central portion of the image; the road leading to the ski area is visible on the lower left part, the ridge of the mountain runs from top to bottom of the image. The largest snow grains, those in the 1700 μm to 2500 μm size range, have been mapped as red. Those ranging in size from about 950 μm to 1690 μm are mapped as blue and the smallest grains in the image, 700 μm to 40 μm, are shown in yellow. As one might expect, there is a grain size gradient which roughly corresponds to elevation, with the largest grains at lower elevations and smaller grains higher up on the mountain. In addition, there seems to be correspondence between grain size and the amount of illumination by diffuse irradiance, with areas of greater illumination being mapped as smaller in size. To provide a better interpretation of the latter problem, the spectral mixing algorithm was applied to a multi-band AVIRIS image. Figure 3 is the fraction of "shade" as determined using endmembers identified in the image (rather than laboratory endmembers). Looking at the Mammoth Mountain part of the image, darker areas correspond to areas of more greater illumination while brighter pixels are those with lower illumination. This is not truly an image of the fraction of shade in each snow-covered pixel, rather it is more a measure of the effect of illumination by both direct and diffuse irradiance on the pixels. In complex topography, sources irradiance are not only the direct and diffuse irradiance from the sun and atmosphere, but direct and diffuse irradiance that has been reflected from topographic facets that face the area of interest. This is a complex modeling problem which has not yet been solved however, the "shade" image may allow us to better interpret and perhaps to calibrate grain size values obtained through this inversion technique.

IV. Conclusions

Our preliminary results show that we can successfully retrieve snowpack properties using high spectral resolution image data. The map of snow grain size which was produced from a single spectral band showed that grain sizes were within the expected physical range for that time of year. As expected, larger grain sizes were at the lower elevations. There also seemed to be a relationship between the amount of diffuse irradiance and the mapped grain size. The "shade" fraction image produced using spectral mixture analysis closely matches grain size patterns on the single band map leading us to believe that this image could provide an empirical means of correction. Clearly, more work needs to be done in this area but these early results are encouraging.

The spectral mixing technique was successful in discriminating between areas of optically thin and thick snow in the Tioga Pass area. Further acquisition of endmember spectra should continue so that we can map other snow types such as wet snow. The nonlinearities which are inherent in the snow mapping problems described in this paper require further investigation.

V. Acknowledgments

This work was supported by NASA grant NAGW-1265. The authors would also like to thank Dr. L.A.K. Mertes for providing access to and assistance with the Washington Image and Spectral Package (WISP) of the University of Washington, Geological Sciences Remote Sensing Laboratory (J. Adams, Director).

REFERENCES

Bohren, C. F., Multiple scattering of light and some of its observable consequences, *Amer. J. Phys.*, *55*, 524-533, 1987.

Chandrasekhar, S., *Radiative Transfer*, Dover Publications, New York, 1960.

Dozier, J., Spectral signature of alpine snow cover from the Landsat Thematic Mapper, *Remote Sens. Environ.*, *28*, 9-22, 1989.

Dozier, J., R. E. Davis, and A. W. Nolin, Reflectance and transmittance of snow at high spectral resolution, *Proceedings IGARSS '89*, 662-664, 1989.

Dubayah, R., The Topographic Variability of Clear-Sky Solar Radiation, Ph.D. Dissertation, 174 pp., Dept. Geogr., Santa Barbara, 1990.

Mugnai, A., and W.J. Wiscombe, Scattering of radiation by moderately nonspherical particles, *J. Atmos. Sci.*, *37*, 1291-1307, 1980.

Nolin, A. W., J. Dozier, and R. E. Davis, Bidirectional reflectance of optically thin snow, *Proceedings IGARSS '90*, 1159, 1990.

Nussenzveig, H. M.,and W. J. Wiscombe, Efficiency factors in Mie scattering, *Phys. Rev. Lett.*, *45*, 1490-1494, 1980.

Warren, S. G.,and W. J. Wiscombe, A model for the spectral albedo of snow, II, Snow containing atmospheric aerosols, *J. Atmos. Sci.*, *37*, 2734-2745, 1980.

Wiscombe, W. J., Improved Mie scattering algorithms, *Appl. Optics*, *19*, 1505-1509, 1980.

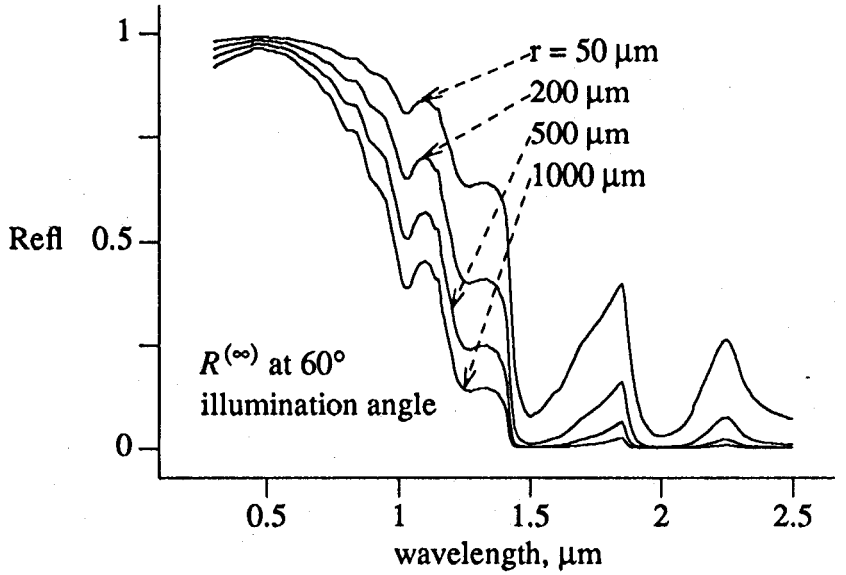

Figure 1. Modeled spectral reflectance of deep snow for different ice grain radii

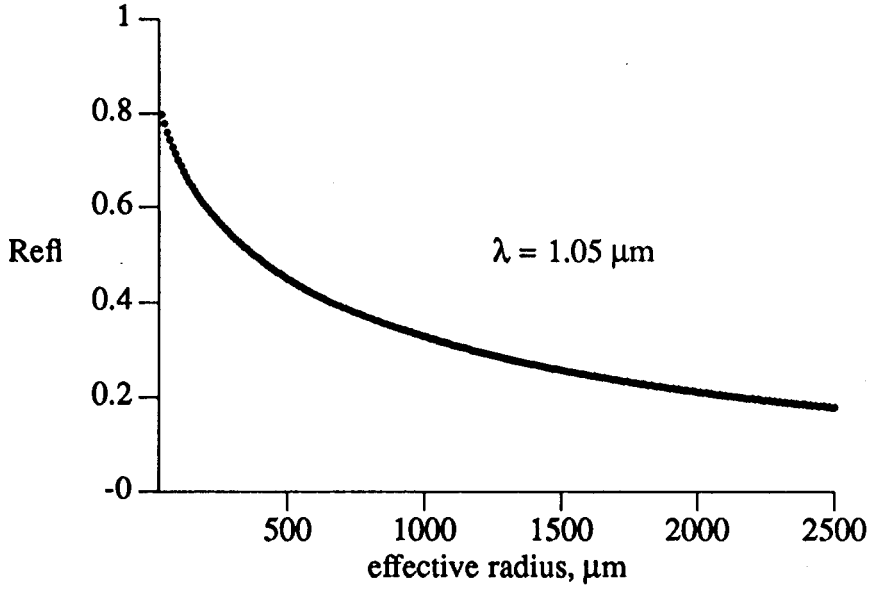

Figure 2. Two-stream model results showing relationship between optically equivalent grain size and snow reflectance

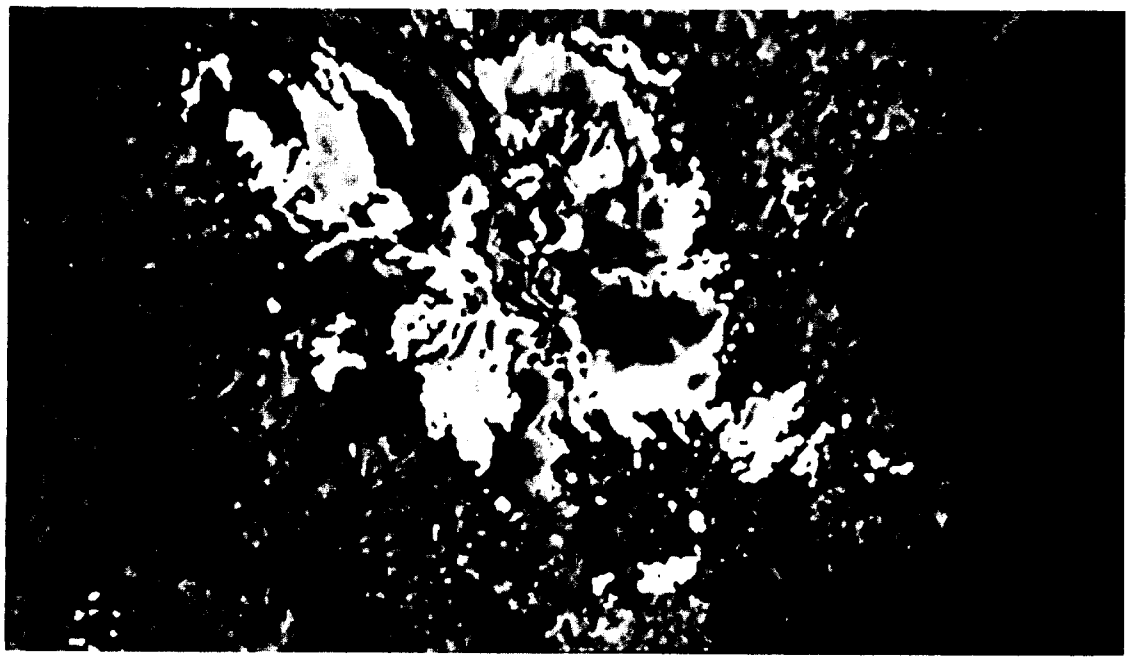

Figure 3. "Shade" fraction image of Mammoth Mountain. North is to the bottom left, solar illumination is from the upper right of the image. Mammoth Mountain is the relatively bright area in the central portion of the image which is bifurcated by a ridge, the dark band running roughly vertically through the middle of the image.